Gauge-Invariant Phase Mapping to Intensity Lobes of Structured Light via Closed-Loop Atomic Dark States.

Nayan Sharma* and Ajay Tripathi
Department of Physics, Sikkim University, 6th Mile Samdur, East Sikkim, India -737102

We present an analytical model showing how the gauge-invariant loop phase in a three-level closed-loop atomic system imprints as bright-dark lobes in Laguerre Gaussian probe beam intensity patterns. In the weak probe limit, the output intensity in such systems include Beer-Lambert absorption, a scattering term and loop phase dependent interference term with optical depth controlling visibility. These systems enable mapping of arbitrary phases via interference rotation and offer a platform to measure Berry phase. Berry phase emerge as a geometric holonomy acquired by the dark states during adiabatic traversal of LG phase defined in a toroidal parameter space. Manifesting as fringe shifts which are absent in open systems, experimental realization using cold atoms or solid state platforms appears feasible, positioning structured light in closed-loop systems as ideal testbeds for geometric phases in quantum optics.

I. INTRODUCTION

Optical light fields with spatially non-unifrom phase, amplitude and polarization known as structured light[1, 2] have emerged as powerful tool in quantum optics. Their applications range from high capacity optical communications[3, 4]and particle trapping[5] to quantum state engineering[6]. Laguerre-Gaussian (LG) beams[7] are one such example distinguished by their helical phase-fronts $e^{il\theta}$ with integer topological charge l. These beams carry orbital angular momentum (OAM)[8] which serves as an extra degree of freedom and offer a high dimensional Hilbert space for encoding quantum information[9].
Closed-loop atomic systems are inherently phase dependent with the existence of phase independent frame determined strictly by the number of independent light fields and the energy levels they couple. These systems are known to exhibit phase dependent effects such as phase dependent electromagnetically induced transparency(EIT)[10–12] and coherent population trapping(CPT)[13]. Nonlinear processes like four-wave mixing[14] and six-wave mixing [15] are also based on such closed-loop systems. The simplest non-trivial configuration is a three-level closed-loop system [16] in which a relative phase remains as a guage-invaraint phase offering an extra handle to probe phase induced effects in light-matter interaction setup.
The synergy between structured light and closed-loop systems have produced valuable results including spatially dependent EIT [17–19], OAM transfer [19–21] and generation of structured light [22–24] explored both experimentally and theoretically. Here, we use this synegry to predict the transfer of the gauge-invariant phase to the intensity lobes of a LG probe beam using a minimal three level closed-loop model. We further disucuss how this platform can map and study the Berry phase [25] which naturally arises from the system's topology making it an excellent platform for such investigations.

* nlop2022@gmail.com

II. TOY MODEL

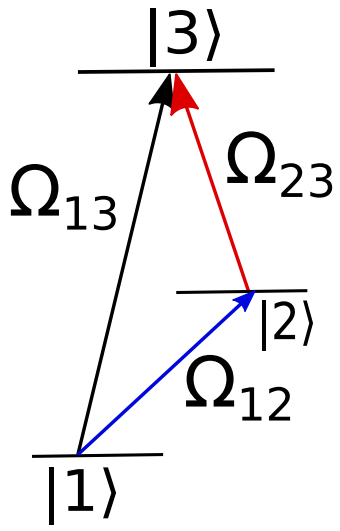

FIG. 1: Schematic of the closed-loop three-level system. The probe beam with Rabi frequency Ω_{13} drives the $|1\rangle \rightarrow |3\rangle$ transition resonantly, while the pump beam with Rabi frequency Ω_{23} couples $|2\rangle \rightarrow |3\rangle$. The loop is closed by the third control field with Rabi frequency Ω_{12} connecting $|1\rangle \rightarrow |2\rangle$. All fields carry phases ϕ_{ij}, enabling mapping of the gauge-invariant loop phase $\Phi = \phi_{12} + \phi_{23} - \phi_{13}$ onto the output intensity pattern.

We consider a three level atomic system $|1\rangle$, $|2\rangle$ and $|3\rangle$ coupled in a closed loop by three light fields, as shown in Fig 1. The probe ($|1\rangle \rightarrow |3\rangle$) is a Laguerre-Gaussian (LG) beam with Rabi frequency $\Omega_{13}(r) = \Omega_0 f_m^{|l|}(r)$, while the pump ($|2\rangle \rightarrow |3\rangle$) is Gaussian $\Omega_{23}(r) = \Omega_c f_0^0(r)$, where

$$f_m^{|l|}(r) = \sqrt{\frac{2m!}{\pi(m+|l|)}} \frac{w_0}{w(z)} \left(\frac{\sqrt{2}r}{w(z)}\right)^{|l|} L_m^{|l|}\left(\frac{2r^2}{w^2(z)}\right) \mathrm{Exp}\left[-\frac{r^2}{w^2(z)} + \frac{ikr^2}{2R(z)} - i\Psi(z)\right] \quad (1)$$

Here, w_0 is the beam waist, $w(z) = w_0\sqrt{1+z^2/z_R^2}$ is the beam radius at point z, $R(z) = z + z_R^2/z^2$ is the wavefront's radius of curvature, $\Psi(z) = (2m+|l|+1)\arctan(z/z_R)$ is the Gouy phase and $z_R = \pi w_0^2/\lambda$ is the Rayleigh range. We consider a regime where the interaction length L $\ll z_R$ in which diffraction effects are neglibigble giving $w(z) \approx w_0$, $R(z) \to \infty$ and $\Psi(z) \approx 0$. The loop is closed with the third beam ($|1\rangle \to |2\rangle$) having Rabi frequency Ω_{12} whose spatial structure is neglected owing to the same no diffraction limit. Further, we assume the weak probe limit ($|\Omega_{13}| \ll |\Omega_{23}|, |\Omega_{12}|$) and resonant (single-photon detunings $\delta_{ij} = 0$) condition. These assumptions enable closed form analytical solutions for the output intensity.

The Hamiltonian for this system in the usual dipole and rotating wave approimation is ($\hbar = 1$),

$$H = \begin{pmatrix} 0 & \Omega_{12}e^{i\phi_{12}} & \Omega_{13}e^{i\phi_{13}} \\ \Omega_{12}e^{-i\phi_{12}} & 0 & \Omega_{23}e^{i\phi_{23}} \\ \Omega_{13}e^{-i\phi_{13}} & \Omega_{23}e^{-i\phi_{23}} & 0 \end{pmatrix} \tag{2}$$

where, $\phi_{13} = l\theta$, θ is the geometric (vortex) phase carried by the LG beam with topological charge $l = 0, \pm1, \pm2, ...$ and ϕ_{12}, ϕ_{23} are the relative phases of the respective coupling beams. This system can be transformed via unitary transformation $UHU^\dagger$ to eliminate the phase dependence, giving a simplified Hamiltonain

$$H' = \begin{pmatrix} 0 & \Omega_{12}e^{i\Phi} & \Omega_{13} \\ \Omega_{12}e^{-i\Phi} & 0 & \Omega_{23} \\ \Omega_{13} & \Omega_{23} & 0 \end{pmatrix} \tag{3}$$

where, $\Phi = \phi_{12} + \phi_{23} - \phi_{13}$ is the unremovable gauge-invaraint loop phase of the system.

The interaction of the beams with the atomic system follows from the optical Bloch equations,

$$\dot{\rho}_{11} = i\Omega_{12}(e^{i\Phi}\rho_{21} - e^{-i\Phi}\rho_{12}) + i\Omega_{13}(\rho_{31} - \rho_{13}) + \Gamma\rho_{33} \tag{4}$$

$$\dot{\rho}_{22} = i\Omega_{12}(e^{-i\Phi}\rho_{12} - e^{i\Phi}\rho_{21}) + i\Omega_{23}(\rho_{32} - \rho_{23}) + \Gamma\rho_{33} \tag{5}$$

$$\dot{\rho}_{12} = i\Omega_{12}(\rho_{22} - \rho_{11})e^{i\Phi} + i\Omega_{13}\rho_{32} - i\Omega_{23}\rho_{13} - \gamma_{12}\rho_{12} \tag{6}$$

$$\dot{\rho}_{13} = i\Omega_{13}(\rho_{33} - \rho_{11}) + i\Omega_{12}e^{i\Phi}\rho_{23} - i\Omega_{23}\rho_{12} - \gamma_{13}\rho_{13} \tag{7}$$

$$\dot{\rho}_{23} = i\Omega_{23}(\rho_{33} - \rho_{22}) + i\Omega_{12}e^{-i\Phi}\rho_{13} - i\Omega_{13}\rho_{21} - \gamma_{23}\rho_{23} \tag{8}$$

with $\rho_{11} + \rho_{22} + \rho_{33} = 1$ and $\rho_{ij}^* = \rho_{ji}$

In the weak probe limit ($\rho_{11} \approx 1, \rho_{22} = \rho_{33} = 0$), the probe coherence becomes

$$\gamma_{13}\rho_{13}(r,\Phi) = \frac{i\gamma_{12}\Omega_{13}(r)}{\Gamma} + \frac{\Omega_{12}\Omega_{23}(r)e^{i\Phi}}{\Gamma} \tag{9}$$

where, γ_{13} and γ_{12} are the decoherence rate for $|1\rangle \to |3\rangle$ and $|1\rangle \to |2\rangle$ respectively and $\Gamma = \gamma_{12} + |\Omega_{23}|^2/\gamma_{13}$. The first term of ρ_{13} (linear in Ω_{13}) represent conventional EIT like coherence, while the second term characterize the closed- loop phase effect.

The propagation equation for the probe beam (in units of γ_{13})is,

$$\frac{d\Omega_{13}(r,z,\Phi)}{dz} = i\alpha\rho_{13}(r,\Phi) \tag{10}$$

with solution

$$\Omega_{13}(r,z,\Phi) = \Omega_{13}(r)e^{-\beta z} + \frac{i\delta}{\beta}(1-e^{-\beta z})e^{i\Phi} \tag{11}$$

where, $\Gamma\beta = 2\alpha\gamma_{12}$, $\Gamma\delta = 2\alpha\Omega_{12}\Omega_{13}$ and α is the on-resonant optical depth per unit length.

The phase of the output probe is,

$$\psi(r,z,\Phi) = \arctan\left(\frac{\Omega_{12}(r)\Omega_{23}(r)(1-e^{-\beta z})\cos(\Phi)}{\gamma_{12}\Omega_{13}(r)e^{-\beta z} - B}\right) \tag{12}$$

where $B = \Omega_{12}(r)\Omega_{23}(r)(1-e^{-\beta z})\sin(\Phi)$ is the interfernce term. The intensity is

$$\mathrm{I}(r,z,\Phi) = \Omega_{13}^2(r)e^{-2\beta z} - \frac{2\Omega_{13}(r)\Omega_{23}(r)\Omega_{12}}{\gamma_{12}}e^{-\beta z} (1-e^{-\beta z})\sin(\Phi) + \frac{\Omega_{23}^2(r)\Omega_{12}^2}{\gamma_{12}^2}(1-e^{-\beta z})^2 \tag{13}$$

The first term represents the coventional Beer-Lambert absorption (valid for open 3-level systems), the second term encodes closed-loop phase modualtion effect and the third term represents a phase-independent scattering term. In principle, the phase-dependent term imprints the dark state information onto the probe intensity pattern, enabling direct extraction of unknown phases Φ through LG beam's output probe intensity profile.

III. DISCUSSION

A. Loop Phase Mapping

Figure 2 shows the input-output (normalized) intensity patterns for LG_0^1 ($l = 1$) probe beam ($\Omega_{13} = \Omega_{12} = 0.1\gamma_{13}$, $\Omega_{23} = 5\gamma_{13}$ and $\phi_{12} + \phi_{23} = 0$). Figure 2 (a) and (b) display the input probe beam intensity and phase variation respectively. After interaction with the atomic system, the output intensity (Fig. 2 (c)) exhibits a bright transmission lobe around $\theta = \pi/2$ and dark lobe at $\theta = 3\pi/2$ expected for $\phi_{12}+\phi_{23} = 0$ where $\Phi = \pi/2, 3\pi/2$ satisfies the dark state condition. The output phase profile is completely changed as compared to the input phase as shown in Fig. 2(d). Figure 3 show similar patterns for LG_0^2 ($l = 2$) probe beam. Figure 3 (a) and (b) display the input intensity and double winding helical phase respectively. The output (Fig. 3(c) and(d)) reveals scattering from the Gaussian pump into the dark vortex, producing an intensity pattern with bright transmission lobes at $\theta = \pi/4, 5\pi/4$ due to the $l = 2$ charge. Notably, the outer ring shows bright lobes at $\theta = 3\pi/4, 7\pi/4$.

We also investigate the output intensity patterns for LG probes at varying optical depth (OD=αL), a crucial

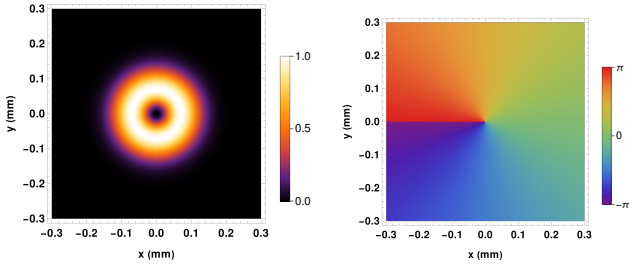

FIG. 2: Azimuthal intensity and phase profiles of LG_0^1 probe beam before and after interaction with the closed-loop system. (a) Input LG_0^1 probe beam intensity with beam waist $w_0 = 100\mu$m with characteristic donut-shaped profile. (b) Input phase structure showing the helical ($l = 1$) azimuthal phase. (c) Output probe beam intensity for optical depth $\alpha L = 1$, Rabi frequencies $\Omega_{13} = \Omega_{12} = 0.1\gamma_{13}$, $\Omega_{23} = 5\gamma_{13}$ and $\phi_{12} + \phi_{23} = 0$ revealing modulation of the dark bright lobes due to interference. (d) Output phase profile of the probe beam.

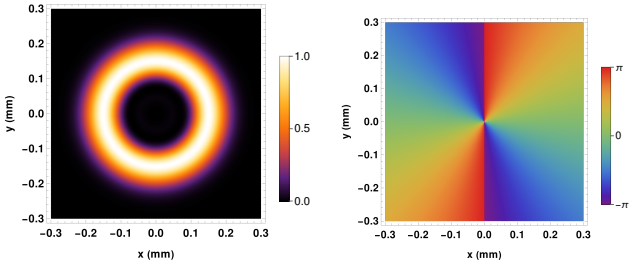

FIG. 3: Azimuthal intensity and phase profiles of LG_0^2 probe beam before and after interaction with the closed-loop system. (a) Input LG_0^2 probe beam intensity with beam waist $w_0 = 100\mu$m with characteristic donut-shaped profile. (b) Input phase structure showing the double helical ($l = 2$) azimuthal phase. (c) Output probe beam intensity for optical depth $\alpha L = 5$, Rabi frequencies $\Omega_{13} = \Omega_{12} = 0.1\gamma_{13}$, $\Omega_{23} = 5\gamma_{13}$ and $\phi_{12} + \phi_{23} = 0$ revealing modulation of the dark bright lobes due to interference. (d) Output phase profile of the probe beam.

parameter for selecting experimental platforms. Figure 4 shows that for LG_0^1, the interference remain clearly resolved at low OD= 0.5 (Fig. 4(a)), but become blurred at high OD of 10 (Fig. 4(b)) due to large scattering. Interestingly for LG_0^2 the fringes are barely discernible at low OD= 1 (Fig. 4(c)) but interference is seen at higher OD = 20 (Fig. 4(d)) reflecting stablity against scattering.

Finally, for completeness, we show the rotation of bight lobes for $LG0^1$ case using two different values of ϕ_{12} (potentially unknown phases). The lobes rotates azimuthally as the value of ϕ_{12} is changed as shown in Fig. 5 (a) and (b). This rotation directly maps unknown loop phases onto observable spatial patterns which could be used for phase metrology via structured light readouts.

B. Berry Phase Mapping

The closed-loop system's gauge-invaraint loop phase ensures that any additional gauge-invariant phase accumulated during slow adiabatic evolution manifests through the intensity maxima-minima as discussed above. To generate non-zero holonomy in the dark state we first examine the energy spectrum via the character-

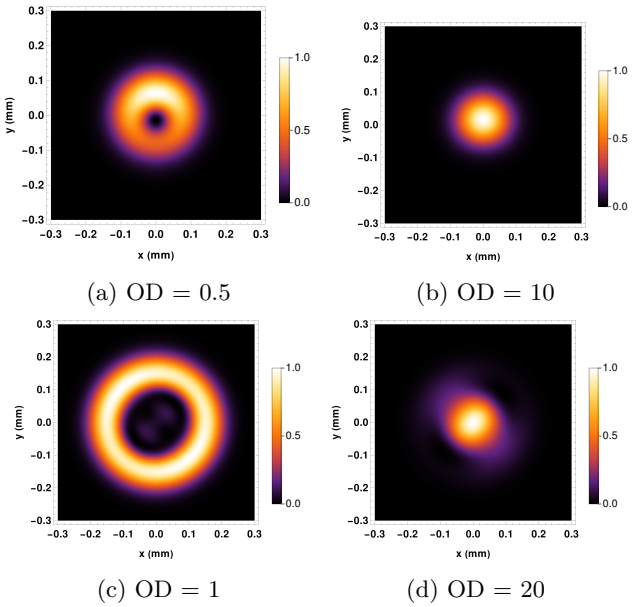

FIG. 4: Output intensity of the probe beam, at different values of optical depth(OD). Panels (a) and (b) correspond to LG_0^1 probe beam while (c) and (d) show results for the LG_0^2 probe beam.

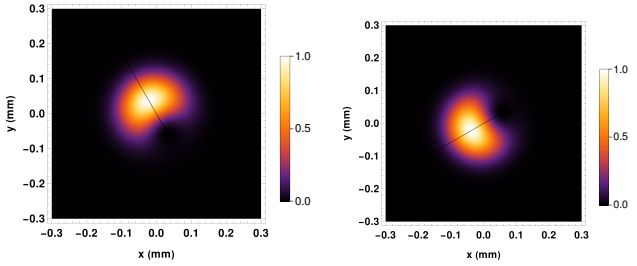

(a) $\phi_{12} = \pi/3$ (b) $\phi_{12} = 5\pi/6$

FIG. 5: Output intensity of the probe beam at two different values of control field phases ϕ_{12} demonstrating sensitivity to unkown phases. Both cases show the rotation of the dark-bright lobes in the intensity pattern.

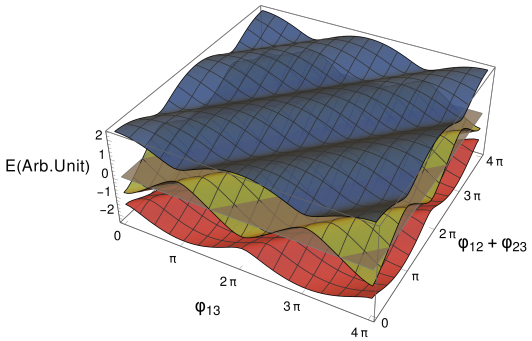

(a) $|\Omega_{12}| \neq |\Omega_{23}| \neq |\Omega_{13}|$

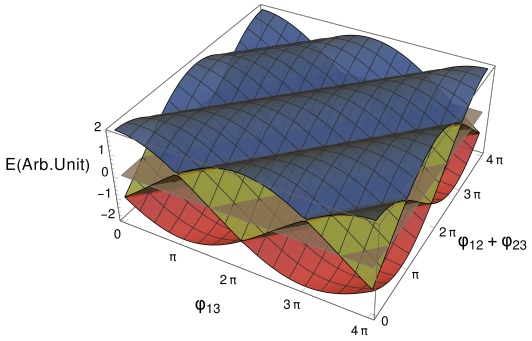

(b) $|\Omega_{12}| = |\Omega_{23}| = |\Omega_{13}$—

FIG. 6: Eigenenergy spectrum as a fucntion of two-dimensional parameter space $(\phi_{12} + \phi_{23}, \phi_{13})$ for (a)the non-degenerate case and (b) degenerate case. The intersection of the plane at E=0 with the energy surface traces the dark-state manifolds.

istic equation of the Hamiltonaian,

$$\Lambda(\Omega_{12}^2 + \Omega_{23}^2 + \Omega_{13}^2 - \Lambda^2) + 2\Omega_{12}\Omega_{23}\Omega_{31}\cos(\Phi) = 0 \quad (14)$$

Dark states $H'|D\rangle = 0$ exist at $\Phi = (2n+1)\pi/2$, while a degenerate eigenspace appears for $\Phi = n\pi$ when $\Omega_{12} = \Omega_{23} = \Omega_{31}$. Figure 6 (a) and (b) shows the energy eigenspectrum in the $(\phi_{12} + \phi_{23}, \phi_{13})$ parameter for

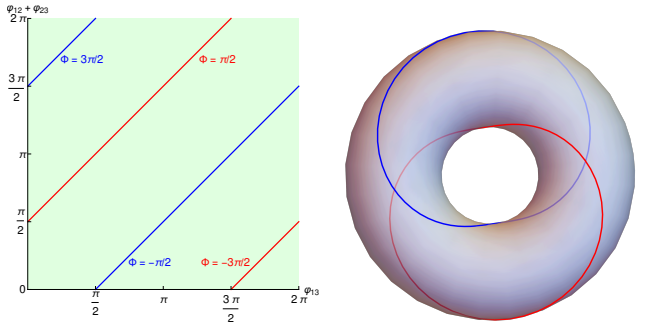

(a) (b)

FIG. 7: Manifold of the dark states in the parameter space $(\phi_{12} + \phi_{23}, \phi_{13})$. (a) Dark states mapped as diagonal line in flat $[0, 2\pi) \times [0, 2\pi)$ parameter space satisfying $\phi_{12} + \phi_{23} - \phi_{13} = \pm\pi/2, 3\pi/2$. (b) These lines map to two non-contractible loops on the torus topology that never cross each other. Adiabatic evolution of the dark state around such a loop acquires a gauge-invariant Berry phase which enters the loop phase Φ and manifests as rotation of interference patterns in the output intensity.

non-degenerate (unequal rabi) and degenerate (equal rabi) cases respectively.

In the non-nondegenerate case for $\Phi = \pi/2, 3\pi/2$, the dark state is

$$|D\rangle = \frac{-i\ \Omega_{23}\,|1\rangle + i\ \Omega_{13}\,|2\rangle + \Omega_{12}\,|3\rangle}{\sqrt{\Omega_{12}^2 + \Omega_{23}^2 + \Omega_{13}^2}} \quad (15)$$

These dark states trace diagonal lines in the phase parameter space $[0, 2\pi) \times [0, 2\pi)$ as shown in Fig.7 (a), which map to two closed loops on the natural torus topology (Fig.7 (b)).

To get a non-zero Berry phase in this system, we suggest the following experimental protocol, which may be implemented with careful parameter control. One could begin by using LG_0^1 probe beam alongside a Gaussian pump to map the loop phase onto intensity lobes and measure the value of the relative phase c(say) (Fig.8 (a)). Subsequently, switching the pump to LG_0^1 beam with a phase profile satifying $\phi_{23} - \phi_{13} = \pi/2 - c$ should ensure $\Phi = \pi/2$ for all azimuthal angles θ, thereby preparing the whole ensemble in the dark state (Fig.8 (b)). From this configuration, adiabatic rotation of the phases in both LG beams might then guide the dark state along one of the non-contractible loops on the torus,

$$|D(\theta(t))\rangle = \frac{-i\ \Omega_{23}e^{i\theta(t)}\,|1\rangle + i\ \Omega_{13}e^{i\theta(t)}\,|2\rangle + \Omega_{12}\,|3\rangle}{\sqrt{\Omega_{12}^2 + \Omega_{23}^2 + \Omega_{13}^2}} \quad (16)$$

Following a full 2π rotation, the Berry phase could then

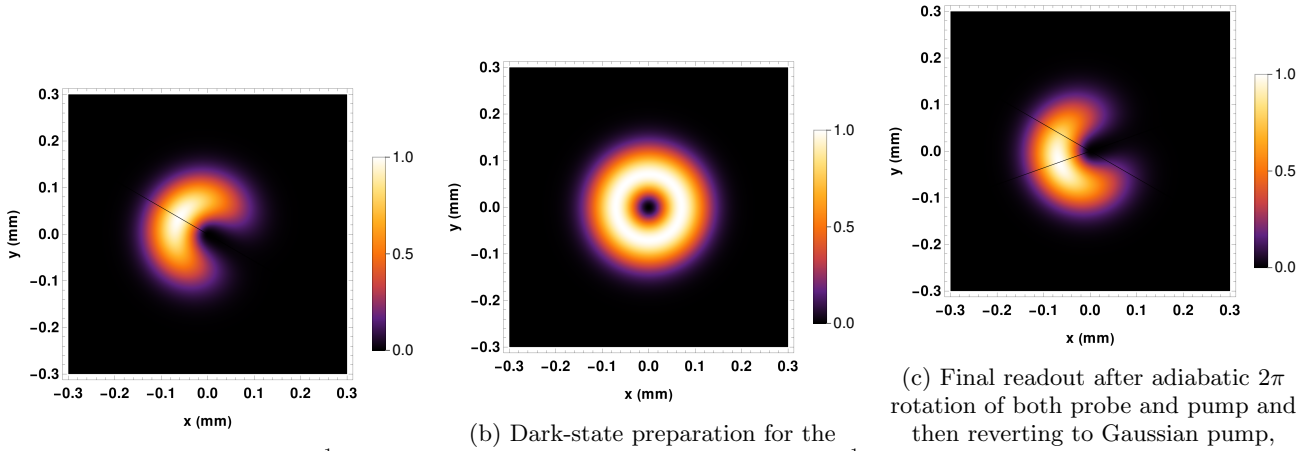

(a) Initial mapping with LG_0^1 probe beam and Gaussian pump, from where an unkown relative phase (say c) can be measured.

(b) Dark-state preparation for the whole ensemble after switching to LG_0^1 pump satisfying $\phi_{23} - \phi_{13} = \pi/2 - c$, ensuring $\Phi = \pi/2$ for all θ which will have no interference term.

(c) Final readout after adiabatic 2π rotation of both probe and pump and then reverting to Gaussian pump, potentailly showing fringe rotation due to accumulated Berry phase (γ_B) observable as shifts in intensity maxima/minima.

FIG. 8: Expected intensity patterns for the proposed Berry phase measurement protocol which may require identifying suitable experimental platforms.

be given by,

$$\gamma_B = i \int_0^{2\pi} d\theta \, \langle D(\theta(t)) | \, \partial_\theta \, | D(\theta(t)) \rangle \tag{17}$$

$$= -2\pi \frac{\Omega_{23}^2 + \Omega_{13}^2}{\Omega_{12}^2 + \Omega_{23}^2 + \Omega_{13}^2} \tag{18}$$

with the dynamical phase vanishing since $H' |D\rangle = 0$ along the loop. Notably, Ω_{12} which is absent in open Λ systems appears responsible for this non-trivial holonomy as $\Omega_{12} \to 0$ recovers $\gamma_B = 0$ for such systems. Finally, reverting to a Gaussian pump may allow readout of γ_B through shifts in the interference fringes, observavble as rotations of intensity maxima and minima (Fig.8 (c)). By tuning the Rabi frequency ratios and ensuring adiabatic looping around the torus, one might thus achieve controllable gauge-invariant phases in this closed-loop geometry.

CONCLUSION

In summary, we have presented a minimal model based analytical caluculations showing how the gauge-invariant loop phase inherent to closed-loop three -level atomic systems can be mapped as the bright dark lobes in the intensity pattern of a structured Laguerre-Gaussian (LG) beams. In the weak probe, no-diffraction limit the output intensity comprises three conbibution, Beer Lambert absorption, scattering and a loop-phase dependent interference term. Our analysis reveals the optical depth as a critical parameter for visibility of the interference. We have shown how these systems may serve as a platform to map arbitrary unknown phase of various sources through controlled rotation of interference patterns. We also proposed a detailed experimental protocol to measure the Berry phase which is geometric gauge-invariant holonomy acquired by the dark state during adaibatic traversal of non-contractible loops on the parameter space defined by LG beam phases in a torus. This phase, which is absent in open Λ systems manifests experimentally as a quantifiable shift in the output interfernce fringes. Experimental realization will require identifying atomic systems where weak probe and adiabatic evolution coexist, along side spatiotemoral control of the light fields. The adiabatic evolution must proceed slowly enough to supress transitions to bright states, yet rapidly enough to preserve coherence against decoherence. These contraints, while challenging, appear within reach using modern cold-atom platforms or solid state systems and appear promising for exploring geometric phases in structured-light quantum optics.

[1] A. Forbes, M. De Oliveira, and M. R. Dennis, Structured light, Nature Photonics **15**, 253 (2021).
[2] H. Rubinsztein-Dunlop, A. Forbes, M. V. Berry, M. R. Dennis, D. L. Andrews, M. Mansuripur, C. Denz, C. Alpmann, P. Banzer, T. Bauer, *et al.*, Roadmap on structured light, Journal of Optics **19**, 013001 (2016).
[3] J. Du and J. Wang, High-dimensional structured light coding/decoding for free-space optical communications free of obstructions, Optics Letters **40**, 4827 (2015).

[4] P. S. Badavath, V. Raskatla, T. P. Chakravarthy, and V. Kumar, Speckle-based structured light shift-keying for non-line-of-sight optical communication, Applied Optics **62**, G53 (2023).

[5] Y. Yang, Y.-X. Ren, M. Chen, Y. Arita, and C. Rosales-Guzmán, Optical trapping with structured light: a review, Advanced Photonics **3**, 034001 (2021).

[6] A. Forbes and I. Nape, Quantum mechanics with patterns of light: progress in high dimensional and multidimensional entanglement with structured light, AVS Quantum Science **1** (2019).

[7] S. Akhtar, M. M. Hossain, and J. K. Saha, Structured light: Study of different profiles of the laguerre-gaussian beam, Resonance **28**, 1359 (2023).

[8] A. E. Willner, Oam light for communications, Optics and Photonics News **32**, 34 (2021).

[9] P. Li, B. Wang, and X. Zhang, High-dimensional encoding based on classical nonseparability, Optics express **24**, 15143 (2016).

[10] E. Korsunsky, N. Leinfellner, A. Huss, S. Baluschev, and L. Windholz, Phase-dependent electromagnetically induced transparency, Physical Review A **59**, 2302 (1999).

[11] A. Joshi, Phase-dependent electromagnetically induced transparency and its dispersion properties in a four-level quantum well system, Physical Review B—Condensed Matter and Materials Physics **79**, 115315 (2009).

[12] H. Li, V. A. Sautenkov, Y. V. Rostovtsev, G. R. Welch, P. R. Hemmer, and M. O. Scully, Electromagnetically induced transparency controlled by a microwave field, Physical Review A—Atomic, Molecular, and Optical Physics **80**, 023820 (2009).

[13] W. Maichen, R. Gaggl, E. Korsunsky, and L. Windholz, Observation of phase-dependent coherent population trapping in optically closed atomic systems, Europhysics Letters **31**, 189 (1995).

[14] M. Ćurčić, T. Khalifa, B. Zlatković, I. Radojičić, A. Krmpot, D. Arsenović, B. Jelenković, and M. Gharavipour, Four-wave mixing in potassium vapor with an off-resonant double-λ system, Physical Review A **97**, 063851 (2018).

[15] Y. Zhang, U. Khadka, B. Anderson, and M. Xiao, Controlling four-wave and six-wave mixing processes in multilevel atomic systems, Applied Physics Letters **91** (2007).

[16] S. Buckle, S. Barnett, P. Knight, M. Lauder, and D. Pegg, Atomic interferometers, Optica Acta: International Journal of Optics **33**, 1129 (1986).

[17] N. Radwell, T. W. Clark, B. Piccirillo, S. M. Barnett, and S. Franke-Arnold, Spatially dependent electromagnetically induced transparency, Physical Review Letters **114**, 123603 (2015).

[18] H. R. Hamedi, V. Kudriašov, J. Ruseckas, and G. Juzeliūnas, Azimuthal modulation of electromagnetically induced transparency using structured light, Optics Express **26**, 28249 (2018).

[19] Rahmatullah, M. Abbas, Ziauddin, and S. Qamar, Spatially structured transparency and transfer of optical vortices via four-wave mixing in a quantum-dot nanostructure, Physical Review A **101**, 023821 (2020).

[20] C. Meng, T. Shui, and W.-X. Yang, Coherent transfer of optical vortices via backward four-wave mixing in a double-λ atomic system, Physical Review A **107**, 053712 (2023).

[21] G. Walker, A. Arnold, and S. Franke-Arnold, Trans-spectral orbital angular momentum transfer via four-wave mixing in rb vapor, Physical review letters **108**, 243601 (2012).

[22] M. Abbas, U. Saleem, Rahmatullah, Y.-C. Zhang, and P. Zhang, Spontaneously generated structured light in a coherently driven five-level m-type atomic system, Physical Review A **109**, 023716 (2024).

[23] O. N. Verma and N. Kant, All-optical generation of structured light beams via microwave-field-controlled electromagnetically induced transparency, Physical Review A **110**, 013701 (2024).

[24] J. A. Thachil, C. R. Patel, O. N. Verma, and A. Kumar, Self-healing of orbital angular momentum in bright twin light beams generated via four-wave mixing, Physical Review A **110**, 053520 (2024).

[25] M. V. Berry, Quantal phase factors accompanying adiabatic changes, Proceedings of the Royal Society of London. A. Mathematical and Physical Sciences **392**, 45 (1984).